

This is the accepted manuscript made available via CHORUS. The article has been published as:

Coupling between phonon and crystal-field excitations in multiferroic $\text{PrFe}_3(\text{BO}_3)_4$

K. N. Boldyrev, T. N. Stanislavchuk, A. A. Sirenko, L. N. Bezmaternykh, and M. N. Popova

Phys. Rev. B **90**, 121101 — Published 2 September 2014

DOI: [10.1103/PhysRevB.90.121101](https://doi.org/10.1103/PhysRevB.90.121101)

Coupling between phonon and crystal-field excitations in multiferroic $\text{PrFe}_3(\text{BO}_3)_4$

K. N. Boldyrev¹, T. N. Stanislavchuk², A. A. Sirenko², L. N. Bezmaternykh³, and M. N. Popova¹

¹*Institute of Spectroscopy, RAS, Moscow, Troitsk, 142190, Russia*

²*Department of Physics, New Jersey Institute of Technology, Newark, New Jersey, 07102, USA*

³*Kirenskiy Institute of Physics, Siberian Branch of RAS, Krasnoyarsk, 660036, Russia*

Abstract

Far infrared reflection and ellipsometry measurements on multiferroic $\text{PrFe}_3(\text{BO}_3)_4$ and $\text{SmFe}_3(\text{BO}_3)_4$ single crystals were used to investigate the interaction between lattice phonons and electronic excitations associated with 4f crystal-field transitions. A temperature-dependent interference between two types of excitations was observed in $\text{PrFe}_3(\text{BO}_3)_4$ in which the frequency of 4f crystal-field electronic excitation of Pr^{3+} falls into the TO – LO frequency interval of the optical phonon mode near 50 cm^{-1} (1.5 THz). Experimental data were explained on the basis of a theoretical model of coupled electron-phonon modes. The fitting procedure revealed the value 14.8 cm^{-1} for the electron-phonon coupling constant. This rather large value points to an essential role played by the electron-phonon interaction in physics of multiferroics.

Keywords: electron-phonon interaction, terahertz spectroscopy, multiferroics, iron borates

PACS numbers: 78.30.-j, 63.20.kd, 75.85.+t, 78.20.Bh

- *Corresponding author. E-mail address: kn.boldyrev@gmail.com*

Introduction. Charge-lattice-spin coupling plays a key role in a vast variety of phases and phenomena observed in multiferroics [1,2]. Pronounced phonon anomalies around the magnetic Neel temperature in multiferroic compounds were demonstrated in Raman scattering (see, e.g., Refs. [3] on BiFeO_3 and [4] on $R\text{CrO}_3$, $R=\text{Gd}, \text{Sm}$) and infrared transmission measurements (of, e.g., $\text{EuFe}_3(\text{BO}_3)_4$ [5]), evidencing the spin-phonon coupling. An anticrossing effect due to the interaction between a crystal-field transition and a magnon was recently observed in the far infrared (FIR) spectra of the multiferroic $\text{Tb}_3\text{Fe}_5\text{O}_{12}$ garnet [6]. As far as we know, no data are available on the interaction of crystal-field electronic excitations with phonons in multiferroics. On the other hand, this type of interactions in concentrated transition-metal or rare-earth (RE) compounds leads to a series of interesting and important phenomena like the cooperative Jahn – Teller effect (for a recent review see Ref. [7]), magnetic phonon splitting [8-10], delocalization of the electronic states in the energy range of optical phonons and, as a consequence, the electronic Davydov splitting [9,11], formation of coupled electron-phonon modes accompanied by a mutual energy renormalization and appearance of new branches in the excitation spectrum [10-16]. Interaction of low-frequency lattice vibrations with CF excitations in RE containing multiferroic compounds can substantially change dispersion of original excitations and cause an onset of new bands in the excitation spectrum, which in its turn can influence magnetodielectric properties of a multiferroic

Here we study the electron-phonon coupling in a multiferroic $\text{PrFe}_3(\text{BO}_3)_4$ single crystal, by means of far infrared (FIR) reflection and ellipsometry measurements. Pronounced spectral signatures of the temperature-dependent electron-phonon interaction were observed. A new effect in optics of the electron-phonon coupling was demonstrated, namely, a splitting of the reflection (“reststrahlen”) band corresponding to a nondegenerate phonon mode. All the observed effects were explained on the basis of theoretical spectra modeling. A value of the electron-phonon coupling constant was found.

Multiferroic $\text{PrFe}_3(\text{BO}_3)_4$ was chosen for these experiments because the energy of the Pr^{3+} lowest excited CF level is very close to the energy of the lowest-frequency infrared-active phonon associated with motions of the R^{3+} ions in $R\text{Fe}_3(\text{BO}_3)_4$ compounds [17-19]. The symmetry requirements for the electron-phonon interaction are also fulfilled (see Supplemental Material [20] for more information on selection rules), so pronounced effects due to the electron-phonon interaction in $\text{PrFe}_3(\text{BO}_3)_4$ could be anticipated when probed by the FIR radiation.

Crystal and magnetic structure. $\text{PrFe}_3(\text{BO}_3)_4$ belongs to the family of new multiferroics with the general formula $R\text{Fe}_3(\text{BO}_3)_4$ (R stands for a rare earth or yttrium). $R\text{Fe}_3(\text{BO}_3)_4$ compounds were intensively studied during recent years because of interesting physical properties and potential applications (see, e.g., Refs. [21-25,17,18]). The $R\text{Fe}_3(\text{BO}_3)_4$ compounds possess a huntite-type noncentrosymmetric trigonal structure that consists of helical chains of edge-sharing FeO_6 octahedra running along the c -axis of the crystal, interconnected by two kinds of BO_3 triangles and RO_6 distorted prisms [26]. In the case of $R\text{Fe}_3(\text{BO}_3)_4$ $R = \text{Pr}$, Nd , and Sm , the structure is described by the $R\bar{3}2$ space group at all the temperatures [25,27,18,28]. There is only one single D_3 symmetry position for the rare-earth (RE) ion in this space group. Crystal-field (CF) levels of a non Kramers ion (i.e., the ion with an even number of electrons, like Pr^{3+}) are characterized by the Γ_1 and Γ_2 nondegenerate and Γ_3 doubly degenerate irreducible representations of the D_3 point symmetry group.

The presence of two interacting magnetic subsystems (Fe and RE) results in a great variety of magnetic and magnetoelectric properties of $R\text{Fe}_3(\text{BO}_3)_4$ compounds, depending on a specific RE ion (see, e.g., Ref. 18 and references therein). In particular, $\text{PrFe}_3(\text{BO}_3)_4$ orders at $T_N = 32 \pm 1$ K into the easy-axis antiferromagnetic structure [27,18]. The low-temperature magnetic and magnetoelectric properties of $\text{PrFe}_3(\text{BO}_3)_4$ are governed, mainly, by the singlet ground Γ_2 and the first excited Γ_1 (at about 48 cm^{-1}) states of the Pr^{3+} ion [27,18,29]. Intermixing of these two lowest CF states by the exchange interaction of Pr^{3+} with an ordered Fe subsystem causes a shift

of the Γ_1 (48 cm^{-1}) level and appearance of forbidden spectral lines of Pr^{3+} in the near infrared and visible spectra below T_N [17].

Experimental details. $\text{PrFe}_3(\text{BO}_3)_4$ and isostructural $\text{SmFe}_3(\text{BO}_3)_4$ (used for comparison) single crystals of good optical quality were grown in the Kirensky Institute of Physics in Krasnoyarsk, as described in Ref. 18. Samples with dimensions $4 \times 4 \times 8 \text{ mm}$ were oriented using the crystal morphology and optical polarization methods. A Fourier spectrometer Bruker IFS 125 HR with a liquid helium bolometer (4.2 K) as a detector and a closed helium cycle cryostat Cryomech ST403 were used to register optical reflectance spectra in the spectral region 0.6 - 3 THz ($20 - 100 \text{ cm}^{-1}$) in the π ($\mathbf{k} \perp c$, $\mathbf{E} \parallel c$, $\mathbf{H} \perp c$) and σ ($\mathbf{k} \perp c$, $\mathbf{E} \perp c$, $\mathbf{H} \parallel c$) polarizations, in a broad range of temperatures (2 – 300 K). FIR ellipsometry measurements were also performed, using self-made ellipsometer on the U4IR beamline of the National Synchrotron Light Source, Brookhaven National Laboratory, USA [30].

Experimental results and discussion. Figures 1(a) and 1(d) show the π -polarized reflection spectra in the region of the lowest frequency A_2^1 phonon of $\text{PrFe}_3(\text{BO}_3)_4$ and $\text{SmFe}_3(\text{BO}_3)_4$, respectively, at several selected temperatures (see Supplemental Material [20] for more information on phonon symmetries and selection rules for optical transitions). Figures 1(b) and 1(c) display the corresponding intensity maps smoothly scanned vs temperature. At room temperature, a strong reststrahlen band typical for a phonon is observed in both compounds. With lowering the temperature, this band does not change in $\text{SmFe}_3(\text{BO}_3)_4$ but splits into two bands (at about 100 K, well above T_N) in $\text{PrFe}_3(\text{BO}_3)_4$. Components of the split band shift in the opposite directions with further lowering the temperature – a gap develops in the spectrum. A pronounced peculiarity in the behavior of both components of the split reflection band of $\text{PrFe}_3(\text{BO}_3)_4$ is observed at the magnetic ordering temperature T_N . If such behavior were a result of a thermal contraction of the crystal or of a phonon anharmonicity close to T_N , it would be observed also in $\text{SmFe}_3(\text{BO}_3)_4$ which has the same crystal structure and the same T_N as

$\text{PrFe}_3(\text{BO}_3)_4$. However, for $\text{SmFe}_3(\text{BO}_3)_4$, the considered phonon mode A_2^1 neither splits nor shifts or shows any peculiarity at T_N [Figs. 1(c), 1(d)]. The only difference between the Sm and Pr compounds is that the lowest CF excitation allowed to interact with the discussed A_2^1 phonon near 50 cm^{-1} lies well above it in $\text{SmFe}_3(\text{BO}_3)_4$ (at 220 cm^{-1} [31]), but falls into its TO – LO interval in $\text{PrFe}_3(\text{BO}_3)_4$. This is a crucial argument in favor of the statement that we observe an interaction between a phonon and an electronic CF excitation in $\text{PrFe}_3(\text{BO}_3)_4$.

Figure 2 displays the real $\langle \varepsilon_1(\omega) \rangle$ and imaginary $\langle \varepsilon_2(\omega) \rangle$ parts of the pseudo-dielectric function of $\text{PrFe}_3(\text{BO}_3)_4$ obtained from the ellipsometry data at different temperatures. Position of the peak in $\langle \varepsilon_2 \rangle$ coincides with the TO frequency, the width is proportional to the damping constant. Figure 2 clearly demonstrates a shift and a narrowing of the quasi-phonon mode with lowering the temperature from RT to $\sim 40 \text{ K}$ and a progressive loss of its intensity below $\sim 40 \text{ K}$. The quasi-electronic mode that appears below $\sim 100 \text{ K}$ (see also Fig. 1), evidently, gains its intensity from the quasi-phonon mode. It should be noted, that purely electronic f - f transitions cannot be observed in reflection, because of their very small oscillator strengths [32]. A pronounced shift of the quasi-electronic mode to higher frequencies is observed below the temperature of an antiferromagnetic ordering T_N [Figs. 1(a), 1(b) and Inset, Fig. 2(b)].

Using the FIR reflection and ellipsometry data, we have extracted the $\omega_{\text{TO}}(T)$ and $\omega_{\text{LO}}(T)$ frequencies (see Supplemental Material [20] for more information) and plotted them on the intensity map of Fig. 1(b) for $\text{PrFe}_3(\text{BO}_3)_4$ and Fig. 1(c) for $\text{SmFe}_3(\text{BO}_3)_4$. A striking difference between the two spectra is evident. Figure 3 shows once more the $\omega_{\text{TO}}(T)$ experimental dependences for the quasi-phonon A_2^1 and the quasi-electronic modes (filled stars) for $\text{PrFe}_3(\text{BO}_3)_4$, to be compared with model calculations.

Modeling Frequencies of coupled electron-phonon excitations can be found as roots of the following equation obtained on the basis of results derived using the Green's functions method in Ref. [33]:

$$\omega^2 - \omega_0^2 + \frac{2\omega_0\omega_{12}(n_1 - n_2)|W|^2}{\omega^2 - \omega_{12}^2} = 0 \quad (1)$$

Here ω_0 and ω_{12} are the frequencies (in cm^{-1}) of the vibrational and electronic excitations, respectively, in the absence of interaction; n_1 and n_2 are relative populations of the excited $|\Gamma_1\rangle$ and ground $|\Gamma_2\rangle$ CF states of Pr^{3+} , respectively; W is the interaction constant between the electronic excitation ω_{12} and the Γ -point A_2^1 optical phonon. This constant determines a change of the RE ion's energy due to a modulation of the crystal field by the A_2^1 lattice vibration. It is possible to show that the interaction constant W is not affected by an intermixing of the $|\Gamma_1\rangle$ and $|\Gamma_2\rangle$ CF states in the internal effective magnetic field created by ordered Fe magnetic moments below T_N . We prove this statement in the Supplemental Material [20]. Solution of Eq. (1) yields:

$$\omega_{\pm}^2 = \frac{\omega_0^2 + \omega_{12}^2}{2} \pm \sqrt{\frac{(\omega_{12}^2 - \omega_0^2)^2}{4} + 2\omega_0\omega_{12}(n_2 - n_1)|W|^2} \quad (2)$$

At high temperatures, $n_1 \approx n_2$, the electron-phonon interaction vanishes, and we have pure phonon and electronic excitations with frequencies $\omega_+ = \omega_{12}$ and $\omega_- = \omega_0$, respectively. Now, we use Eq. 2 to fit the experimental data of Fig. 3. The temperature-dependent position $\omega_{12}(T)$ of the Pr^{3+} crystal-field level was found earlier from optical spectroscopy data [17,18], it is represented by balls in Fig. 3. In the case of the Boltzman distribution of populations of electronic levels, the difference of populations $n_1 - n_2$ is given by $n_1 - n_2 = \tanh \frac{\omega_{12}(T)}{2kT}$. The interaction constant $|W|$ and the original phonon frequency ω_0 at 300 K, $\omega_0(300K)$, were varied to achieve the best agreement with the experimental data. Besides, a linear softening of ω_0 with decreasing the temperature was introduced, $\omega_0 = \omega_0(300K) - k(300K - T)$, to account for other than electron-phonon interaction mechanisms (e.g., changes of particular interatomic distances in a crystal and, hence, force constants with cooling or an interaction of this phonon mode with the spin system, due to a modulation of Fe-O-Fe angles by a given vibration [34]). The σ -polarized $E(xy)$ phonon

mode near 84 cm^{-1} , also shown in Fig. 3 (open stars), or the A_2^1 phonon mode in $\text{SmFe}_3(\text{BO}_3)_4$ [Fig. 1 (c)] demonstrate examples of an almost linear mode softening with lowering the temperature. The simulated curves (with $|W|=14.8 \text{ cm}^{-1}$, $\omega_0(300\text{K})=45.2 \text{ cm}^{-1}$, $k=0.019 \text{ cm}^{-1}/\text{K}$) are plotted in Fig. 3. A good agreement with the experimentally measured temperature dependences of the TO frequencies is evident. Being compared with unperturbed frequencies ω_0 and ω_{12} , the frequencies of the coupled electron-phonon modes ω_- and ω_+ clearly demonstrate a mutual "repulsion" [Fig.3].

Thus, the used theoretical model of the electron-phonon coupling describes the experimental data reasonably well. It should be mentioned that the observed splitting of a reflection band corresponding to a *nondegenerate* phonon mode of $\text{PrFe}_3(\text{BO}_3)_4$ (or, in other words, a gap formation in the spectrum of excitations) can be considered as a new effect in physics of the electron-phonon interaction. A gap in the spectrum of elementary excitations due to repulsion of dispersion curves of the electronic and phonon systems (the so called "anticrossing" effect) was previously observed in a series of different experiments. In Raman scattering and infrared absorption or reflection measurements that probe the $k = 0$ point of the Brillouin zone, the anticrossing and transfer of transition intensities between components of the coupled electron-phonon excitations were observed via tuning of an electronic level into a resonance with a phonon, by an external magnetic field [10-12,16]. In neutron scattering experiments at a constant magnetic field (which determined an energy of the lowest crystal-field excitation), repulsed dispersion curves $\omega_1(k)$ and $\omega_2(k)$ were measured directly and the wave-vector dependence of the electron-phonon interaction was studied [13]. Here we observe a new effect of this type. A gap in the spectrum of excitations develops with lowering the temperature, due to a growing interaction between a *nondegenerate* optical phonon and an electronic 4f crystal-field excitation, the frequency of which falls into the region between TO and LO frequencies of the phonon. In

the Supplemental Material [20] we analyze a gap formation in more detail, by analogy with earlier examined case of two phonons.

Summary. To summarize, we combined reflection and ellipsometry measurements in the FIR (terahertz) frequency region and a theoretical simulation to study electron-phonon coupling in a multiferroic $\text{PrFe}_3(\text{BO}_3)_4$ single crystal. An isostructural $\text{SmFe}_3(\text{BO}_3)_4$ single crystal was also investigated for comparison. A special feature of $\text{PrFe}_3(\text{BO}_3)_4$ is that the lowest-frequency Pr^{3+} crystal-field excitation falls into the region between the TO and LO frequencies of a strong lattice phonon mode of the same symmetry as the electronic excitation. Pronounced spectral peculiarities due to the electron-phonon interaction were observed and explained. In particular, a new effect was demonstrated, namely, a splitting of the reststrahlen band corresponding to a nondegenerate phonon mode. A rather large value of about 15 cm^{-1} for the electron-phonon coupling constant found from numerical simulation points to an essential role played by the electron-phonon interaction in physics of multiferroics.

Acknowledgements. Research supported by the Russian Scientific Foundation under Grant No 14-12-01033, the President of Russian Federation (MK-1700.2013.2, K.N.B.), and the U.S. Department of Energy under Grant No DE-FG02-07ER46382 (experiments at U4-IR beamline NSLS-BNL, T.N.S. and A.A.S.). The National Synchrotron Light Source is operated as a User Facility for the U.S. Department of Energy under Contract No. DE-AC02-98CH10886. M.N.P. thanks B.Z. Malkin for drawing her attention to the work [33] and for helpful discussions.

References:

- [1] S. W. Cheong and M. Mostovoy, *Nature Materials*, **6**, 13 (2007).
- [2] J. van den Brink, D. Khomskii, *J. Phys.: Condens. Matter* **20**, 434217 (2008).
- [3] R. Haumont, J. Kreisel, P. Bouvier, and F. Hippert, *Phys. Rev. B* **73**, 132101 (2006).
- [4] V. S. Bhadram, R. Rajeswaran, A. Sundaresan, and C. Narayana, *EPL*, **101**, 17008 (2013).

- [5] K. N. Boldyrev, T. N. Stanislavchuk, S. A. Klimin, M. N. Popova, and L. N. Bezmaternykh, *Phys. Lett. A* **376**, 2562 (2012).
- [6] T. D. Kang, E. Standard, K. H. Ahn, A. A. Sirenko, G. L. Karr, S. Park, Y. J. Choi, M. Ramazanoglu, V. Kiryukhin, and S. W. Cheong, *Phys. Rev. B* **82**, 014414 (2010).
- [7] M. Kaplan, “Cooperative Jahn-Teller Effect: Fundamentals, Applications, Prospects”, in *The Jahn-Teller Effect*, Editors: Horst Köppel, David R. Yarkony, Heinz Barentzen (Springer, Berlin, Heidelberg, 2009) Springer Series in Chem. Physics, Vol. 97, pp.653-683 (2009)
- [8] K. Ahrens and G. Schaack, *Phys. Rev. Lett.* **42**, 1488 (1979).
- [9] M. Dahl and G. Schaack, *Phys. Rev. Lett.* **56**, 232 (1986).
- [10] A. K. Kupchikov, B. Z. Malkin, A. L. Natadze, and A. I. Ryskin, *Fiz. Tverd. Tela* **29**, 3335 (1987) [*Sov. Phys. Solid State* **29**, ... (1987)].
- [11] J. Kraus, W. Görlitz, M. Hirsch, R. Roth, and G. Schaack, *Z. Phys. B – Condensed Matter* **74**, 247 (1989).
- [12] A. K. Kupchikov, B. Z. Malkin, A. L. Natadze, and A. I. Ryskin. Spectroscopy of electron-phonon excitations in rare-earth crystals. In *Spectroscopy of crystals* (in Russian), Nauka, Leningrad, 1989, pp. 84-112.
- [13] J. K. Kjems, W. Hayes, and S. H. Smith, *Phys. Rev. Lett.* **35**, 1089 (1975).
- [14] S. Guitteny, J. Robert, P. Bonville, J. Ollivier, C. Decorse, P. Steffens, M. Boehm, H. Mutka, I. Mirebeau, and S. Petit, *Phys. Rev. Lett.* **111**, 087201 (2013).
- [15] T. Fennell, M. Kenzelmann, B. Roessli, H. Mutka, J. Ollivier, M. Ruminy, U. Stuhr, O. Zaharko, L. Bovo, A. Cervellino, M. K. Haas, and R. J. Cava, *Phys. Rev. Lett.* **112**, 017203 (2014).
- [16] T. V. Brinzari, J. T. Haraldsen, P. Chen, Q.-C. Sun, Y. Kim, L.-c. Tung, A. P. Litvinchuk, J. A. Schlueter, D. Smirnov, J. L. Manson, J. Singleton, and J. L. Musfeldt, *Phys. Rev. Lett.* **111**, 047202 (2013).

- [17] M. N. Popova, T. N. Stanislavchuk, B. Z. Malkin, and L. N. Bezmaternykh, *Phys. Rev. Lett.* **102**, 187403 (2009).
- [18] M. N. Popova, T. N. Stanislavchuk, B. Z. Malkin, and L. N. Bezmaternykh, *Phys. Rev. B* **80**, 195101 (2009).
- [19] K. N. Boldyrev and D. A. Erofeev, *Optika i Spektroskopiya* **116**, 67 (2014) [*Opt. Spectrosc.* **116**, 872 (2014)].
- [20] See Supplemental Material at <http://link.aps.org/supplemental/.....> for (a) symmetry analysis of crystal-field excitations and phonons, of selection rules for optical transitions and for the electron-phonon interaction, (b) dispersion analysis applied to find phonon parameters, (c) analysis of the temperature dependence of the electron-phonon interaction constant, (d) analysis of a gap formation in the spectrum of excitations.
- [21] F. Yen, B. Lorenz, Y. Y. Sun, C. W. Chu, L. N. Bezmaternykh, and A. N. Vasiliev, *Phys. Rev. B* **73**, 054435 (2006).
- [22] R. P. Chaudhury, F. Yen, B. Lorenz, Y. Y. Sun, L. N. Bezmaternykh, V. L. Temerov, and C. W. Chu, *Phys. Rev. B* **80**, 104424 (2009).
- [23] U. Adem, L. Wang, D. Fausti, W. Schottenhamel, P. H. M. van Loosdrecht, A. Vasiliev, L. N. Bezmaternykh, B. Büchner, C. Hess, and R. Klingeler, *Phys. Rev. B* **82**, 064406 (2010).
- [24] A. I. Popov, D. I. Plokhov, and A. K. Zvezdin, *Phys. Rev. B* **87**, 024413 (2013).
- [25] D. Fausti, A. Nugroho, P. H. M. Loosdrecht, S. A. Klimin, M. N. Popova, and L. N. Bezmaternykh, *Phys. Rev. B* **74**, 024403 (2006).
- [26] N. I. Leonyuk and L. I. Leonyuk, *Progr. Cryst. Growth Charact.* **31**, 179 (1995).
- [27] A. M. Kadomtseva, Yu. F. Popov, G. P. Vorob'ev, A. A. Mukhin, V. Yu. Ivanov, A. M. Kuz'menko, and L. N. Bezmaternykh, *JETP Lett.* **87**, 39 (2008).
- [28] E. P. Chukalina, M. N. Popova, L. N. Bezmaternykh, and I. A. Gudim, *Phys. Lett. A* **374**, 1790 (2010).

- [29] N. V. Kostyuchenko, A. I. Popov, A. K. Zvezdin, Fiz. Tverd. Tela **54**, 1493 (2012) [Phys. Solid State **54**, 1591 (2012)].
- [30] T. N. Stanislavchuk, T. D. Kang, P. D. Rogers, E. C. Standard, R. Basistyy, A. M. Kotelyanskii, G. Nita, T. Zhou, G. L. Carr, M. Kotelyanskii, and A. A. Sirenko, Rev. Sci. Instr. **84**, 023901 (2013).
- [31] M. N. Popova, E. P. Chukalina, B. Z. Malkin, D. A. Erofeev, L. N. Bezmaternykh and I. A. Gudim, Z. Eksp. Teor. Fiz. **145**, 128 (2014) [JEPT **118**, 111 (2014)].
- [32] G. H. Dieke, “Spectra and Energy Levels of Rare Earth Ions in Crystals”, Interscience Publishers: New York 1968.
- [33] A. K. Kupchikov, B. Z. Malkin, D. A. Rzaev, and A. I. Ryskin, Fiz. Tverd. Tela **24**, 2373 (1982) [Sov. Phys. Solid State **24**, 1348 (1982)]. It should be emphasized that in the case of crystal excitations the method of local coupled oscillators used, e.g. in [16], is not valid. In particular, it overlooks the dependence of the interaction value on the population difference $n_1 - n_2$.
- [34] A. B. Kuz'menko, D. van der Marel, P. J. M. van Bentum, E. A. Tishchenko, C. Presura, and A. A. Bush, Phys. Rev. B **63**, 094303 (2001).

Figure captions

FIG. 1 (color online). The π -polarized FIR reflection spectra and the corresponding reflection intensity maps in the frequency-temperature axes for (a,b) $\text{PrFe}_3(\text{BO}_3)_4$ and (c,d) $\text{SmFe}_3(\text{BO}_3)_4$, $T_N = 32 \pm 1$ K for both compounds. (b,c) Navy-blue (dark) stars represent ω_{TO} frequencies, blue (gray) points denote ω_{LO} frequencies. A splitting of the $\text{PrFe}_3(\text{BO}_3)_4$ reststrahlen band near 50 cm^{-1} below ~ 100 K is seen.

FIG. 2 (color online). The real $\langle \epsilon_1(\omega) \rangle$ and imaginary $\langle \epsilon_2(\omega) \rangle$ parts of the pseudo-dielectric function of $\text{PrFe}_3(\text{BO}_3)_4$ obtained from the ellipsometry data at different temperatures. Insets show an expanded view of the emerging high-frequency branch of the spectrum.

FIG. 3 (color online). Temperature dependences of the TO frequencies extracted from the FIR reflection and ellipsometry data for $\text{PrFe}_3(\text{BO}_3)_4$ (filled stars). Small black balls interconnected with a dashed line represent the temperature-dependent position ω_{12} of the Pr^{3+} crystal-field level found earlier from optical spectroscopy data [18]. A straight dashed line corresponds to the unperturbed phonon frequency ω_0 used in model calculations. The calculated (from Eq. 2) TO frequencies ω_+ and ω_- of the coupled electron-phonon modes are shown by green open circles and thick lines for the following set of parameters: $|W| = 14.8 \text{ cm}^{-1}$, $\omega_0(300\text{K}) = 45.2 \text{ cm}^{-1}$, $k = 0.019 \text{ cm}^{-1}/\text{K}$ (for details, see the text). Experimental data on the TO frequency of the lowest $E(\text{xy})$ phonon mode of $\text{PrFe}_3(\text{BO}_3)_4$ (open stars) are shown for a comparison.

Figures

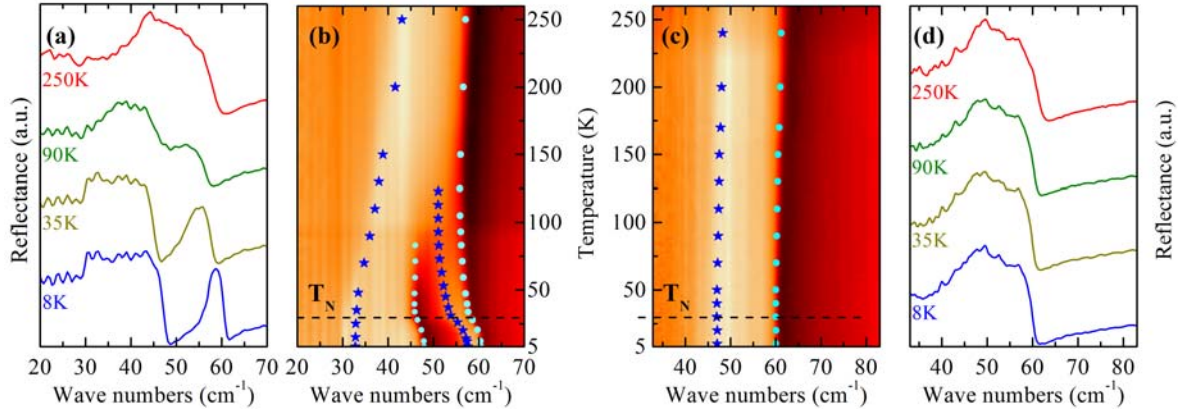


FIG. 1 (color online). The π -polarized FIR reflection spectra and the corresponding reflection intensity maps in the frequency-temperature axes for (a,b) $\text{PrFe}_3(\text{BO}_3)_4$ and (c,d) $\text{SmFe}_3(\text{BO}_3)_4$, $T_N = 32 \pm 1$ K for both compounds. (b,c) Navy-blue (dark) stars represent ω_{TO} frequencies, blue (gray) circles denote ω_{LO} frequencies. A splitting of the $\text{PrFe}_3(\text{BO}_3)_4$ reststrahlen band near 50 cm^{-1} below ~ 100 K is seen.

Please note that this is a double column figure

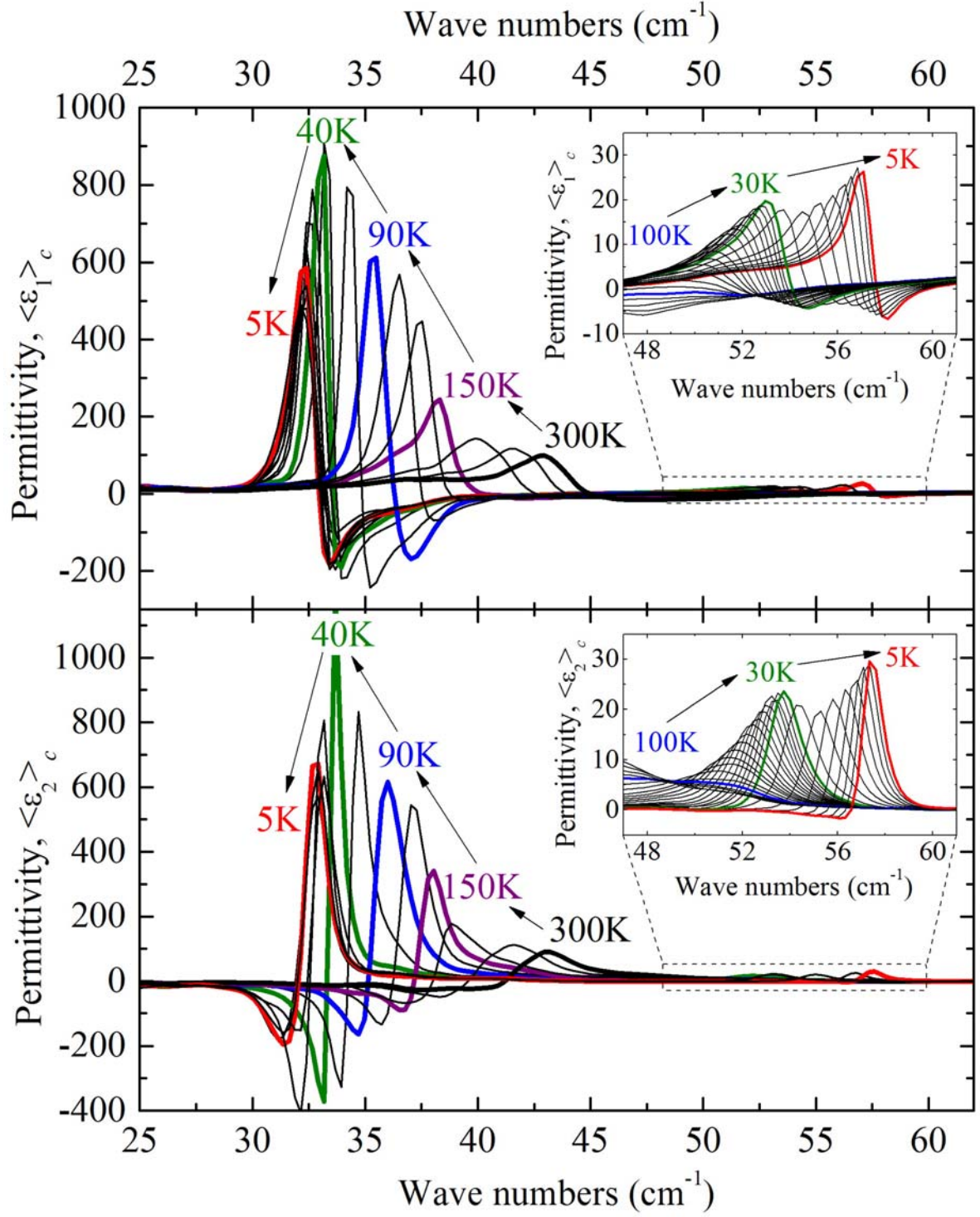


FIG. 2 (color online). The real $\langle \epsilon_1(\omega) \rangle$ and imaginary $\langle \epsilon_2(\omega) \rangle$ parts of the pseudo-dielectric function of $\text{PrFe}_3(\text{BO}_3)_4$ obtained from the ellipsometry data at different temperatures. Insets show an expanded view of the emerging high-frequency branch of the spectrum.

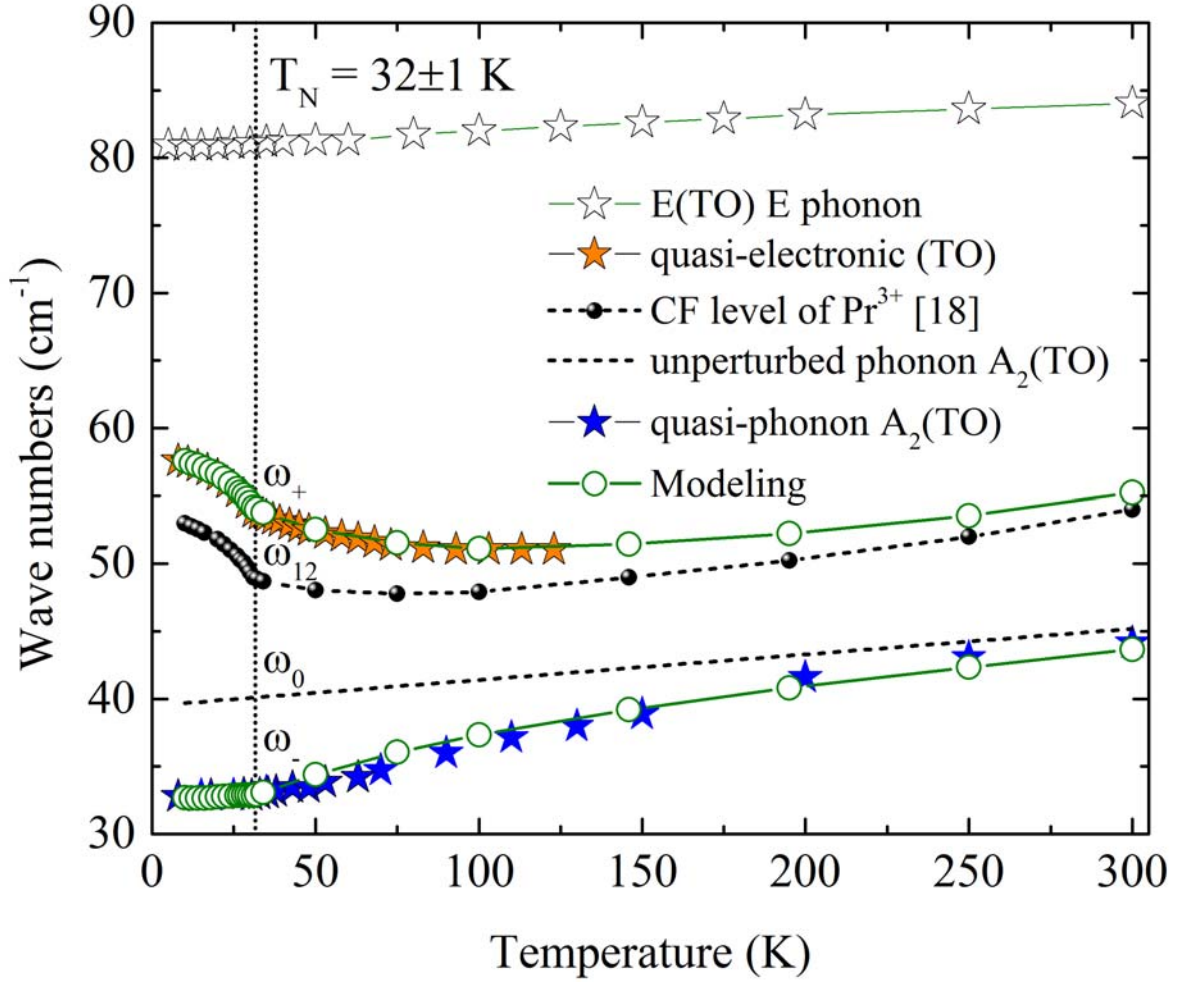


FIG. 3 (color online). Temperature dependences of the TO frequencies extracted from the FIR reflection and ellipsometry data for $\text{PrFe}_3(\text{BO}_3)_4$ (filled stars). Small black balls interconnected with a dashed line represent the temperature-dependent position ω_{12} of the Pr^{3+} crystal-field level found earlier from optical spectroscopy data [18]. A straight dashed line corresponds to the unperturbed phonon frequency ω_0 used in model calculations. The calculated (from Eq. 2) TO frequencies ω_+ and ω_- of the coupled electron-phonon modes are shown by green open circles and thick lines for the following set of parameters: $|W| = 14.8 \text{ cm}^{-1}$, $\omega_0(300\text{K}) = 45.2 \text{ cm}^{-1}$, $k = 0.019 \text{ cm}^{-1}/\text{K}$ (for details, see the text). Experimental data on the TO frequency of the lowest $E(xy)$ phonon mode of $\text{PrFe}_3(\text{BO}_3)_4$ (open stars) are shown for comparison.